

Temperature Dependence of the Reaction between O(³P) and OClO at Low Pressure

James F. Gleason,^{*,†} Fred L. Nesbitt,[‡] and Louis J. Stief[†]

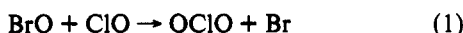
Laboratory for Extraterrestrial Physics, NASA/Goddard Space Flight Center, Greenbelt, Maryland 20771

Received: February 26, 1993; In Final Form: August 27, 1993[•]

The rate coefficient for the reaction O(³P) + OClO has been measured at low pressure (1–5 Torr) over the temperature range 200–400 K. The experiments were performed in a discharge flow system with atomic resonance fluorescence detection of O(³P). The ratio of [OClO]/[O] was kept very high (usually 10³–10⁴) in order to avoid secondary reactions. At 298 K, $k = (1.0 \pm 0.3) \times 10^{-13}$ molecule⁻¹ cm³ s⁻¹, which is consistent with recent results obtained at high pressure (8–800 Torr argon) and extrapolated to zero pressure. In the present low-pressure experiments, the rate coefficient increases with increasing temperature from 243 to 400 K while from 200 to 225 K the rate coefficient decreases with increasing temperature. The Arrhenius expression for the 243–400 K region is $k = (2.4 \pm 0.8) \times 10^{-12} \exp[(-960 \pm 120)/T]$ molecule⁻¹ cm³ s⁻¹. The trend observed here for $T = 243$ –400 K is opposite to that inferred from the extrapolation of high-pressure results (20–600 Torr argon) at $T = 248$ –312 K. Our high-temperature results (243–400 K) are consistent with the bimolecular abstraction channel, O(³P) + OClO → ClO + O₂.

Introduction

Recent observations of OClO in both the Antarctic^{1–3} and Arctic^{4–6} polar stratosphere have renewed interest in the chemistry of this molecule. The observations indicate enhanced levels of stratospheric chlorine, which are associated with stratospheric ozone destruction. The primary source of stratospheric OClO is the reaction⁷



OClO is a link between the Cl and Br cycles in the stratosphere, and the analysis of the OClO diurnal variation has been used to calculate the relative contributions of different proposed ozone destruction mechanisms.^{7–8} The use of a molecule, like OClO, as a tracer species requires that all of its sources and sinks be well characterized. Although photolysis is expected to be the major atmospheric loss process for OClO, potential chemical loss processes have not been well studied. At the time we initiated this work, rate coefficients had been measured for the reaction of OClO with Cl,⁹ O(³P),⁹ H,⁹ NO,⁹ Br,¹⁰ OH,¹¹ SO,¹² and O₃.^{13,14} Although the temperature dependence of the rate coefficients have been determined for the Cl, OH, and O₃ reactions, only room-temperature data were available for the O(³P), H, Br, NO, and SO reactions. Of these, the most interesting for atmospheric science is probably the reaction



The reaction is slow at room temperature:⁹ k_2 (298 K) = $(5_{-2}^{+1}) \times 10^{-13}$ molecule⁻¹ cm³ s⁻¹. With a reasonable estimated positive temperature dependence for an abstraction reaction,¹⁵ the reaction would be unimportant under stratospheric conditions. However, the recent demonstration by Colussi¹⁶ that the reaction shows a very significant pressure effect at 298 K emphasizes the need to determine the temperature dependence of k_2 . The temperature dependence of the low-pressure rate coefficient would provide insight into whether the reaction has two independent channels (bimolecular and termolecular pathways) or proceeds solely via a collision-complex mechanism.

The reaction between O(³P) and OClO may also be significant in complex laboratory studies designed to reveal the spectra,

photochemistry, and chemical reactivity of Cl oxides such as the ClO dimer (ClO)₂ and the molecule Cl₂O₃, especially those that use OClO as a starting material.^{17,18}

In these experiments we have undertaken a study of the reaction O(³P) + OClO at low pressure (1–5 Torr He) in order to determine the temperature dependence of the absolute rate coefficient from 200 to 400 K.

Experimental Section

The experiments were performed in a discharge flow reactor using resonance fluorescence and mass spectrometric detection. The basic apparatus has been described previously,¹⁹ and only the modifications made for this experiment will be described. A four-way cross was added to the end of the flow tube for the resonance fluorescence detection. Oxygen atom resonance radiation at $\lambda = 130$ nm was produced by passing He with trace amounts of O₂ through a 2450-MHz microwave discharge. The light from the resonance lamp, with a MgF₂ window, was uncollimated and used a series of 6-mm baffles to reduce the amount of scattered light entering the flow tube. The resonantly scattered photons were detected by a baffled solar blind PMT with a 1-mm CaF₂ cutoff filter ($\lambda > 120$ nm) at right angles to the resonance lamp. The oxygen atoms were produced by passing low concentrations of O₂ in He through a 2450-MHz microwave discharge. Typical O(³P) atom concentrations were in the range 5–8 × 10¹⁰ molecules cm⁻³ and were determined by measuring mass spectrometrically the change in the O₂ concentration with the microwave discharge on and off, i.e. $[\text{O}] = 2 \times \Delta[\text{O}_2]$.

The OClO was prepared by a standard method and purified as described by Toohey.²⁰ In summary, Cl₂ was passed through a U-tube containing sodium chlorite (NaClO₂) supported on glass beads. The OClO was collected in a cold finger at 223 K and purified by the following bulb to bulb distillation procedure. The residual Cl₂ was removed by pumping on the OClO held at 223 K, and the liquid OClO was then warmed to 243 K and distilled into a second cold finger immersed in liquid nitrogen. This procedure removed any traces of H₂O or higher Cl oxides. A waxy orange solid and some white ice frost was usually left in the first cold finger. The second cold finger was warmed to 243 K, and the middle fraction of this second distillation was collected in the first cold finger, immersed in liquid nitrogen. The OClO from this three-step procedure was stored at 193 K when not in use. The use of unpurified OClO directly from the NaClO₂

[†] NASA/NRC Resident Research Associate. Present address: Laboratory for Atmospheres, NASA/Goddard Space Flight Center, Mail Code 916, Greenbelt, MD 20771.

[‡] Also at: Department of Natural Science, Coppin State College, Baltimore, MD.

[•] Abstract published in *Advance ACS Abstracts*, December 1, 1993.

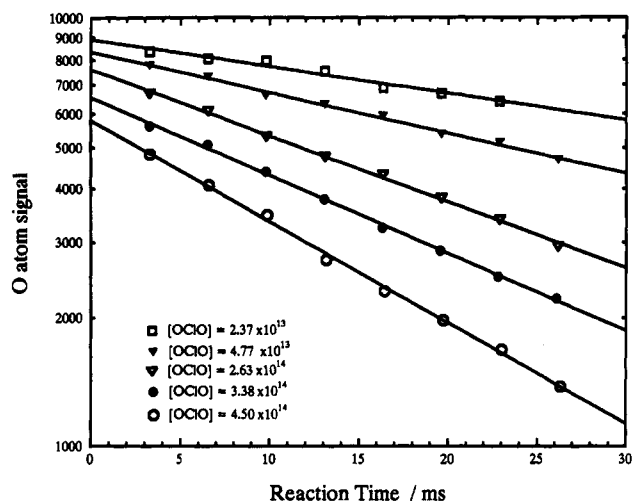


Figure 1. O atom signal vs reaction time at pressure = 1.1 Torr and $T = 298$ K; [OCIO] units are molecules cm^{-3} .

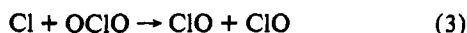
generator gave nonreproducible results. The purified material can be quite unstable and should be handled with extreme caution. We had two spontaneous decompositions of OCIO, both resulting in equipment damage and personal injury. The cause of the explosions has not been identified, so the amount of purified material should be kept to a minimum to reduce this hazard.

The flow of the reagent OCIO was determined by two methods. High concentrations (20–40% OCIO/He) were used in the initial experiments. The total flow of the mixture was monitored using a calibrated mass flow controller, and the OCIO concentration was determined by optical absorption at $\lambda = 405$ nm. These mixtures showed no loss of OCIO over a 6-h period. The optical setup consisted of a low-pressure Hg lamp, absorption cell, and 0.2-nm monochromator coupled to a photomultiplier tube. The OCIO cross section was taken from Wahner et al.,²⁰ $\sigma(405 \text{ nm}) = 2.19 \times 10^{-18} \text{ cm}^2$. The flow controller readings were unstable at higher concentrations (>40%) of OCIO. In the second method we used the vapor from the top of pure OCIO liquid in a thermostated bath. The flow of pure OCIO, from a calibrated volume, was determined for each experiment by measuring $\Delta P / \Delta T$ while OCIO was continuously monitored by optical absorption. The flow of pure OCIO was pushed into the flow reactor by a small additional flow of He gas.

The experiments were performed by monitoring the decay of the O atom resonance signal as a function of the position of the movable injector. The concentration of OCIO is changed, and the process is repeated (see Figure 1). The decay of the atomic oxygen is represented by $\ln[\text{O}]_t = -k_{\text{obs}}t + \ln[\text{O}]_0$, where the pseudo-first-order rate coefficient k_{obs} is given by $k_{\text{obs}} = k_2[\text{OCIO}] + k_{\text{wall}}$. The slope of each decay line plotted as a function of the OCIO concentration yields the second-order rate coefficient for reaction 2, at that temperature and pressure. The gases used were UHP grade and used without additional purification.

Results

The rate coefficient for reaction 2 was measured under pseudo-first-order conditions with $[\text{OCIO}] \gg [\text{O}]_0$. As a check on the modified apparatus and on the quantitative handling of OCIO, we first measured the rate coefficient for the reaction



Formation of the ClO product from reaction 3 was observed via collision-free sampling mass spectrometry using low-energy electron impact ionization. In addition, we observed Cl_2O_3 as a product of subsequent reaction of the ClO product with the OCIO reactant. For the study of reaction 3, we monitored the decay

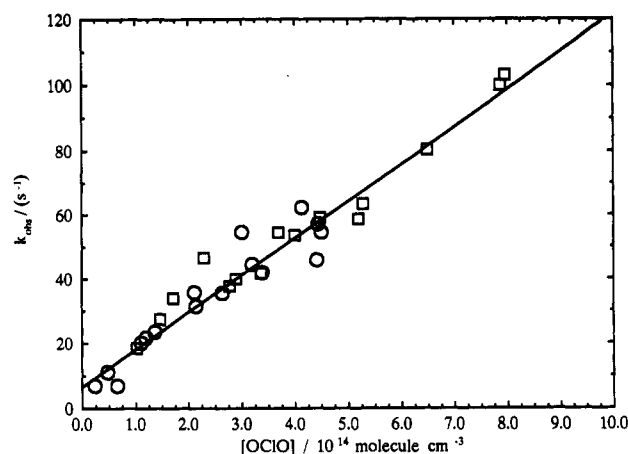


Figure 2. k_{obs} vs [OCIO] for O(³P) + OCIO at $T = 298$ K. The open circles represent data taken at 1 Torr. The open squares are data taken at 5 Torr. The line is the least-squares fit to the 1 Torr data.

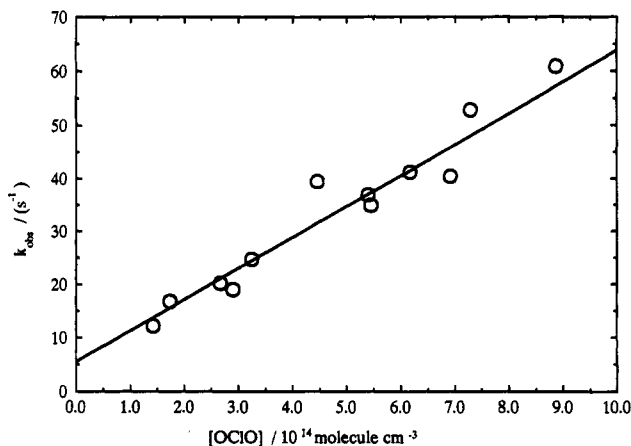


Figure 3. k_{obs} vs [OCIO] for O(³P) + OCIO at $T = 200$ K. Symbols represent the data, and the line is the least-squares fit.

of Cl using resonance fluorescence under pseudo-first-order conditions. We performed six experiments with $[\text{Cl}] = 1 \times 10^{11} \text{ molecule cm}^{-3}$ and $[\text{OCIO}] = 3\text{--}8 \times 10^{12} \text{ molecule cm}^{-3}$. Our result, $k_3(298 \text{ K}) = (6.6 \pm 1.2) \times 10^{-11} \text{ molecule}^{-1} \text{ cm}^3 \text{ s}^{-1}$, is in excellent agreement with the only published determination of the rate coefficient, $k_3 = (5.9 \pm 0.9) \times 10^{-11} \text{ molecule}^{-1} \text{ cm}^3 \text{ s}^{-1}$.⁹

The rate coefficient for reaction 2 was measured over a wide temperature range, 200–400 K. The bulk of the experiments were conducted at about 1 Torr total pressure. Additional experiments were conducted at a higher pressure (5 Torr, 298 K). The experimental first-order decay constant, k_{obs} , was obtained from the slope of the plot of the $\ln(\text{O atom signal})$ vs reaction time. Typical decays are shown in Figure 1. Corrections to k_{obs} to allow for axial diffusion of O(³P) atoms in the He carrier gas proved to be quite small (<4%) and were neglected. A plot of the pseudo-first-order rate coefficient k_{obs} vs [OCIO] is shown in Figure 2 for reaction 2 at $T = 298$ K. These results exhibit good linearity with a statistically insignificant intercept of 6 s^{-1} . The bimolecular rate coefficient obtained from these results is $k_2(298 \text{ K}) = (1.0 \pm 0.3) 10^{-13} \text{ molecule}^{-1} \text{ cm}^3 \text{ s}^{-1}$. The quoted uncertainty includes statistical errors at the $\pm\sigma$ level plus an additional 12% to allow for propagation of error due to uncertainties in [OCIO], total flow of gases, total pressure, reaction temperature, and flow tube radius. The largest of these errors is the uncertainty in [OCIO].

The lack of a pressure dependence can be seen in Figure 2. There is no significant difference in the rate coefficient data that can be attributed to the effect of pressure between 1 and 5 Torr He. This is consistent with the extrapolated Ar data from Colussi,¹⁶ which predict at most only a 10–15% change between

TABLE 1: Summary of Rate Data for the O + OCIO Reaction

<i>T</i> /K	<i>P</i> /Torr	[OCIO]/10 ¹⁴ molecule cm ⁻³	<i>k</i> _{obs} /s ⁻¹ ^a	<i>T</i> /K	<i>P</i> /Torr	[OCIO]/10 ¹⁴ molecule cm ⁻³	<i>k</i> _{obs} /s ⁻¹ ^a		
400	1.3	1.57	33.4 ± 1.2	263	1.2	3.96	33.1 ± 1.2		
		0.844	17.8 ± 1.7			6.62	50.3 ± 1.5		
		4.51	98.1 ± 3.1			1.61	20.5 ± 0.8		
		2.62	42.4 ± 0.5			9.23	59.9 ± 2.0		
345	1.2	<i>k</i> (400 K) ^b = (2.15 ± 0.58) × 10 ⁻¹³ molecule ⁻¹ cm ³ s ⁻¹		243	1.3	<i>k</i> (263 K) ^b = (5.98 ± 1.05) × 10 ⁻¹⁴ molecule ⁻¹ cm ³ s ⁻¹			
		2.90	60.6 ± 1.4			9.59	54.5 ± 0.8		
		5.35	90.5 ± 2.4			2.18	21.3 ± 0.7		
		0.988	22.9 ± 2.2			4.58	32.8 ± 0.8		
		1.75	39.8 ± 3.2			5.79	42.6 ± 1.4		
300	1.1	<i>k</i> (345 K) ^b = (1.53 ± 0.34) × 10 ⁻¹³ molecule ⁻¹ cm ³ s ⁻¹		225	1.3	<i>k</i> (243 K) ^b = (4.54 ± 0.89) × 10 ⁻¹⁴ molecule ⁻¹ cm ³ s ⁻¹			
		4.43	57.1 ± 0.6			4.99	30.3 ± 0.6		
		3.19	44.4 ± 0.9			6.89	38.3 ± 0.9		
		2.11	35.7 ± 1.1			2.88	21.0 ± 1.0		
		1.10	20.1 ± 0.8			7.54	40.9 ± 1.0		
		4.13	62.2 ± 2.0			12.3	66.7 ± 1.7		
		3.00	54.5 ± 1.3			<i>k</i> (225 K) ^b = (4.28 ± 0.56) × 10 ⁻¹⁴ molecule ⁻¹ cm ³ s ⁻¹			
		1.36	23.5 ± 1.0			212	1.2	5.73	29.1 ± 1.0
		0.660	7.0 ± 1.2					8.60	45.2 ± 0.8
		2.14	31.4 ± 2.0					1.93	13.6 ± 0.7
		4.50	54.5 ± 1.0					12.3	66.7 ± 1.7
		3.38	41.8 ± 0.7					<i>k</i> (212 K) ^b = (5.14 ± 0.93) × 10 ⁻¹⁴ molecule ⁻¹ cm ³ s ⁻¹	
		2.63	35.5 ± 0.7					200	1.3
	1.19	21.7 ± 0.7	5.40	36.9 ± 1.3					
	0.477	11.1 ± 0.5	8.87	60.9 ± 3.7					
	0.237	7.0 ± 1.0	7.29	52.9 ± 1.0					
	3.63	34.1 ± 1.0	1.73	16.8 ± 0.5					
	4.41	45.8 ± 1.3	4.46	39.4 ± 1.3					
	1.71	33.9 ± 0.7	2.90	19.0 ± 0.3					
	2.89	39.9 ± 1.8	1.42	12.2 ± 0.6					
	4.47	59.1 ± 2.9	6.92	40.4 ± 1.7					
	3.69	54.4 ± 2.2	5.45	34.9 ± 0.8					
	2.29	46.5 ± 1.4	6.17	41.2 ± 1.3					
	7.86	100 ± 5	2.67	20.2 ± 0.7					
	6.49	80.4 ± 3.2	10.36	62.6 ± 1.4					
	7.95	103 ± 7	<i>k</i> (200 K) ^b = (5.90 ± 1.11) × 10 ⁻¹⁴ molecule ⁻¹ cm ³ s ⁻¹						
	5.19	58.6 ± 1.5							
4.00	53.5 ± 2.0								
2.77	37.7 ± 0.5								
1.46	27.4 ± 0.8								
8.04	78.5 ± 1.7								
5.28	63.4 ± 1.7								
3.36	41.7 ± 2.2								
1.02	18.5 ± 0.7								
		<i>k</i> (300 K) ^b = (1.05 ± 0.33) × 10 ⁻¹³ molecule ⁻¹ cm ³ s ⁻¹							

^a Statistical uncertainty only (±1σ). ^b Uncertainty is ±1σ plus allowance for accumulation of errors in [OCIO], pressure, temperature, etc. See text.

these He pressures. This small of an effect would be difficult to measure with this reaction system.

Figure 3 is a plot of *k*_{obs} vs [OCIO] at *T* = 200 K. The results exhibit good linearity with a statistically insignificant intercept of 5 s⁻¹. The bimolecular rate coefficient obtained from the results is *k*₂(200 K) = (5.9 ± 1.1) × 10⁻¹⁴ molecule⁻¹ cm³ s⁻¹, where the quoted uncertainty is estimated as described above for *k*₂(298 K).

Table 1 summarizes all the rate data for the O(³P) + OCIO reaction. Several reaction parameters and conditions were varied. These included variation of [OCIO]₀/[O]₀ from 400 to 20 000, variation of [OCIO] by a factor of 50, and variation of the total pressure from 1 to 5 Torr. The [O] was kept very low (<10¹¹ molecules cm⁻³) to avoid any secondary chemistry, and hence only a minimal (~ factor of 2) variation in [O] was possible. None of these variations had any effect on the observed reaction kinetics.

A plot of ln(*k*₂) vs 1000/*T* from *T* = 200 to 400 K is shown in Figure 4. The temperature dependence observed is different from the usual Arrhenius form. The rate coefficient increases with increasing temperature from 243 to 400 K, while from 200 to 225 K the rate coefficient decreases with increasing temperature. The total measured rate coefficient, *k*₂, may be represented as a sum of two terms which have a positive and negative

temperature dependence, respectively,

$$k_2 = A_1 \exp(-E_1/RT) + A_2 \exp(-E_2/RT) \quad (I)$$

Although the small increase in *k*₂ at the lowest temperatures and the small temperature interval may not yield realistic Arrhenius parameters, *A*₂ and *E*₂, it is necessary to allow for the second term in arriving at *A*₁ and *E*₁ for the first term. A nonlinear least-squares fit of all the data (*T* = 200–400 K) yields the following parameters for the first term: *A*₁ = (2.43 ± 0.84) × 10⁻¹² molecule⁻¹ cm³ s⁻¹, *E*₁/*R* = 962 ± 122 K. The quoted errors are statistical only at the 2σ level. The parameters for the second term (given here for completeness) are empirical and not mechanistically interpretable: *A*₂ = 1.5 × 10⁻¹⁹ molecule⁻¹ cm³ s⁻¹, *E*₂/*R* = -2500 K. An alternate estimate of *A*₁ and *E*₁/*R* may be obtained by neglecting the three low-temperature points and fitting the *T* = 243–400 K data to the simple expression

$$k_2 = A_1 \exp(-E_1/RT) \quad (I')$$

This yields *A*₁ = (2.59 ± 0.26) × 10⁻¹² molecule⁻¹ cm³ s⁻¹ and *E*₁/*R* = 981 ± 74 K, where again the errors are at the 2σ level. It is clear that this estimate is well within the uncertainty for both *A*₁ and *E*₁/*R* from the full data analysis using equation I. We prefer the complete analysis and thus quote *k*₂ for *T* = 243–400 K as *k*₂ = (2.4 ± 0.8) × 10⁻¹² exp[(-960 ± 120)/*T*] molecule⁻¹

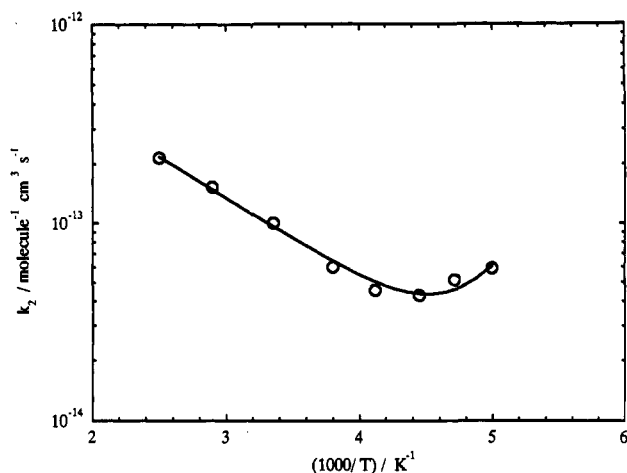


Figure 4. Arrhenius plot for k_2 . Symbols represent the data, and the line is the least-squares fit.

$\text{cm}^3 \text{s}^{-1}$. These parameters can be associated with the bimolecular abstraction channel which dominates at higher temperatures.

Discussion

The present DF-RF result of k_2 (298 K) = $(1.0 \pm 0.3) \times 10^{-13}$ molecule⁻¹ cm³ s⁻¹ at 1–5 Torr He is much lower than the DF-RF/MS result of Bemand et al.⁹ ($5.2^{+1} \times 10^{-13}$ molecule⁻¹ cm³ s⁻¹ at ~ 1 Torr He, even allowing for the large error limits for the latter results. An important contribution of the Bemand et al. study⁹ was the demonstration that the rate coefficient for reaction 2 was much slower than suggested by previous, less direct determinations. Specifically, they showed that when $[\text{OCIO}]_0/[\text{O}]_0$ was < 100 in the resonance fluorescence experiments, the initial O(³P) + OCIO reaction was followed by the rapid reactions O(³P) + ClO and Cl + OCIO



$$k_2 = 1 \times 10^{-13} \text{ molecule}^{-1} \text{ cm}^3 \text{ s}^{-1} \quad (2)$$



$$k_4 = 4 \times 10^{-11} \text{ molecule}^{-1} \text{ cm}^3 \text{ s}^{-1} \quad (4)$$



$$k_3 = 6 \times 10^{-11} \text{ molecule}^{-1} \text{ cm}^3 \text{ s}^{-1} \quad (3)$$

This results in an autocatalytic cycle which consumes both O(³P) and OCIO, and large apparent decay rates are observed for both reactants.

Our values for k_2 (298 K) at 1–5 Torr He are reasonably consistent with the recent high-pressure results (8–800 Torr argon) of Colussi,¹⁶ extrapolated to zero pressure, i.e., k_2 (298 K) = $(1.6 \pm 0.4) \times 10^{-13}$ molecule⁻¹ cm³ s⁻¹. It should be noted that, in Colussi's flash photolysis experiments, the observed O atom decay rates were dependent on the incident excimer laser intensity, i.e., on initial [O]. This is clear evidence for the occurrence of the autocatalytic cycle (reactions 4 and 3) identified by Bemand et al.⁹ To correct for this, Colussi determined the apparent rate coefficient k_2 as a function of $[\text{O}]_0/[\text{OCIO}]$ and extrapolated to $[\text{O}]_0/[\text{OCIO}] = 0$. The reasonable agreement between his low-pressure bimolecular rate coefficient value, corrected for secondary chemistry, and our 1 Torr value, determined in the absence of secondary chemistry ($[\text{OCIO}]/[\text{O}]_0 = 10^4$), demonstrates the essential correctness of this approach. A further point of interest from his k vs $[\text{O}]_0/[\text{OCIO}]$ plot, not noted by Colussi, is that at $[\text{O}]_0/[\text{OCIO}] = 0.01\text{--}0.005$ (reproducing the best conditions of the experiments of Bemand et al.) the observed rate coefficient is $k_2 = 5 \times 10^{-13}$ molecule⁻¹ cm³ s⁻¹, similar to the value measured

by Bemand et al. The implication of the lower result obtained by Colussi and by us ($k_2 = 1.0 \times 10^{-13}$ molecule⁻¹ cm³ s⁻¹) and the observation that Colussi's results show a dependence of the observed rate coefficient on the $[\text{OCIO}]/[\text{O}]_0$ ratio, even when the ratio is as large as 200, is that the results of Bemand et al., despite their identification and awareness of the autocatalytic cycle, were still determined under conditions ($[\text{OCIO}]/[\text{O}] = 135$) where secondary reactions were occurring.

The temperature dependence of the bimolecular rate coefficient measured in this low-pressure study from 243 to 400 K may be compared with that estimated in the 1990 NASA data evaluation.¹⁵ The assumed value $E/R = 1200$ K was a reasonable approximation on the basis of our measured value $E/R = 960$ K. The estimated preexponential A factor is of course high (by about a factor of 10) since it was chosen to reproduce the high rate constant value of Bemand et al.⁹ The more recent 1992 NASA data evaluation²² is based on our results. The dominant reaction mechanism in this temperature and pressure regime is almost certainly a simple O atom abstraction with an energy barrier (1.9 kcal/mol) and a somewhat low A factor (2.4×10^{-12} molecules⁻¹ cm³ s⁻¹).

A very recent study of the effect of temperature (248, 273, and 312 K) and total pressure (20–600 Torr argon) by Colussi, Sander, and Friedl²³ provides direct information on the pressure-dependent rate coefficient k_{ter} but only indirect information on the pressure-independent rate coefficient k_{bi} . The best fit of their experimental results for k_{bi} , obtained by a rather uncertain extrapolation of the overall k vs total pressure plots to zero pressure, leads to the expression

$$k_{\text{bi}} = 1.86 \times 10^{-13} (T/300)^{-4.35} \text{ molecule}^{-1} \text{ cm}^3 \text{ s}^{-1} \quad (\text{II})$$

Thus, at the three temperatures of their experiments, the extrapolated bimolecular rate coefficient values are k_2 (312 K) = 1.6×10^{-13} , k_2 (273 K) = 2.8×10^{-13} , and k_2 (248 K) = 4.3×10^{-13} , all in units of molecule⁻¹ cm³ s⁻¹. It is clear that these rate constant values at 273 and 248 K are significantly larger than ours and that k_{bi} increases with decreasing temperature from 312 to 248 K, a trend opposite to that observed in the present experiments from 400 to 243 K.

Our results are consistent with the flash photolysis results^{16,23} at 298 and 312 K and disagree with their results at the two lower temperatures, 248 and 273 K. We consider our results to be a better measure of the bimolecular channel. The difference may be caused by secondary chemistry in the flash experiments. Any secondary chemistry, possibly from ClO formed in the flash, will cause the observed rate constant to be higher than the actual rate coefficient. The second-order rate constants from the flash experiments¹⁶ at 298 K have shown a dependence on flash energy. The Colussi room-temperature experiments used a model of the secondary chemistry, including many temperature-dependent reactions, to extrapolate their observed values to zero flash energy. The flash extrapolations from the room-temperature paper show that the lower pressure measurements are significantly noisier and show a greater flash energy dependence. In the temperature-dependent study, the experiments showing the dependence on flash energy were not reported in their paper. Figure 5 shows an attempted synthesis of the pressure dependence of the O + OCIO reaction at four temperatures. We used our values for k_{bi} (1 and 5 Torr) and the Colussi et al.^{16,23} values for k_0 and k_{∞} (20–600 Torr). The points are the experimental data (not available for the 298 K study¹⁶), and the lines are those calculated from the expression^{23,24}

$$k = k_{\text{bi}} + k_{\infty} \{r[\text{M}]/(1 + r[\text{M}])\} F_c^{1 + [\log(r[\text{M}])/N]^2} \quad (\text{III})$$

where $r = k_0/k_{\infty}$, M is the third body, F_c is the broadening factor, and N is the width factor (see ref 23, eqs 7 and 8, as well as the original Troe formula in ref 24). Figure 5 shows that there is a significant change in slope in the experiments below 50 Torr.

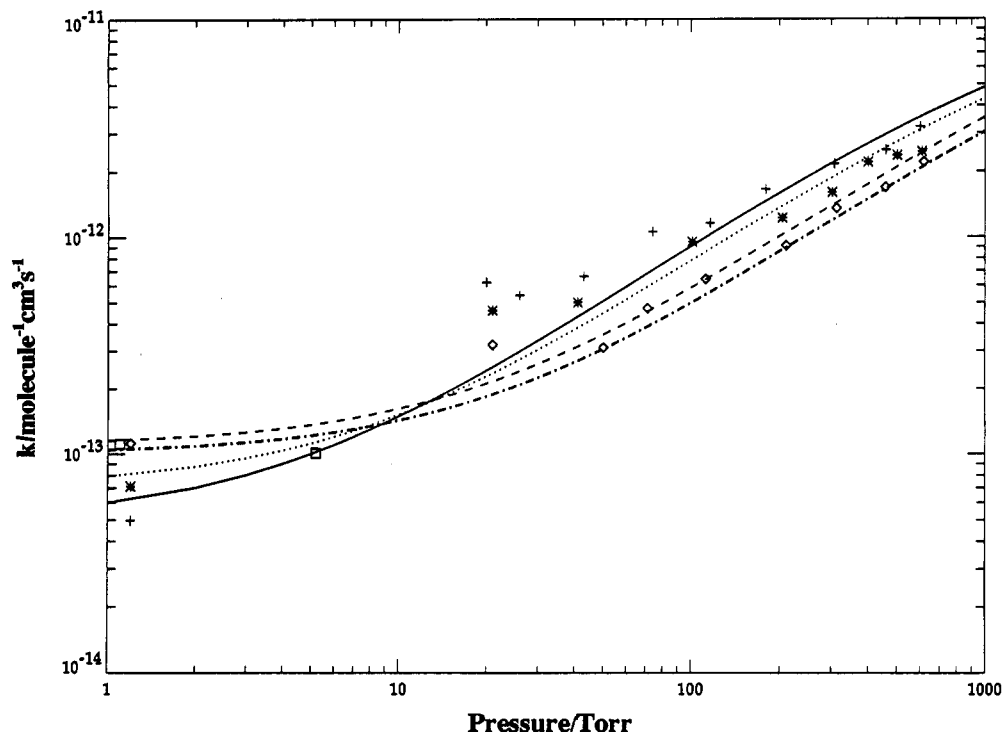
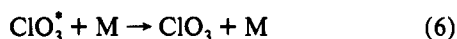


Figure 5. Pressure dependence of the rate constant for the O + OClO reaction at four temperatures. Lines represent fit to equation III in the text: (—) 248 K, (···) 273 K, (---) 312 K, (-·-) 298 K. Symbols represent data points: (+) 248 K, (*) 273 K, (◇) 312 K, (□) 298 K. Individual data points at 298 K are not available for the 20–760 Torr experiments.²³

This slope change was not observed in the 298 K experiments. Their minimum flash energy may be too high at low temperature and lower pressures, leading to a higher rate coefficient. There is not sufficient experimental data reported in the Colussi et al. paper to check for secondary chemistry.

The positive temperature dependence for the bimolecular channel observed here supports the occurrence of a direct abstraction reaction at low pressure rather than decomposition of the ClO₃ intermediate to the products ClO and O₂.

The small negative temperature dependence of the rate coefficient observed by us between $T = 225$ and 200 K qualitatively supports the suggestion by Colussi¹⁶ and Colussi, Sander, and Friedl,²³ based on extensive documentation of a pressure-dependent process, that an additional process is occurring



The best fit of their pressure-dependent data at $T = 248, 273,$ and 312 K yields the expression

$$k_{\text{ter}} = (1.86 \times 10^{-31})(T/300)^{-1.12} \text{ molecule}^{-2} \text{ cm}^6 \text{ s}^{-1} \quad (\text{IV})$$

Since we could not detect a pressure effect over our limited pressure range (nor do their data require one) and since we only detected a small increase in k_2 ($(4.3\text{--}5.9) \times 10^{-14} \text{ molecule}^{-1} \text{ cm}^3 \text{ s}^{-1}$) over a small temperature interval (225–200 K), our experiments provide no quantitative information on the termolecular process.

The rate parameters for the O(³P) + OClO reaction may be compared with those for the similar O(³P) + NO₂ reaction. Both reactions involve two primary channels: a bimolecular path involving abstraction of atomic oxygen (yielding O₂ and ClO or NO) and a termolecular path involving addition and stabilization of the ClO₃ and NO₃ intermediate. The results are summarized in Table 2 along with the appropriate references. For the bimolecular channel, the O(³P) + NO₂ reaction is nearly 2 orders of magnitude faster at 298 K than the O(³P) + OClO reaction. This is due largely to the activation energy for O(³P) + OClO, the preexponential A factors differing only by about a factor of

TABLE 2: Comparison of Bimolecular and Termolecular Reactions of O(³P) Atoms with OClO and NO₂

bimolecular reaction	$k(298 \text{ K})^a$	A^a	E/R	ref
O(³ P) + OClO → ClO + O ₂	1.0×10^{-13}	2.4×10^{-12}	960	this work
O(³ P) + NO ₂ → NO + O ₂	9.7×10^{-12}	6.5×10^{-12}	-120	DeMore et al. ¹⁵
termolecular reaction	$k_0(298 \text{ K})^b$	n	$k_{\infty}(298 \text{ K})^c$	ref
O(³ P) + OClO → ClO ₃	1.9×10^{-31}	1.12	3.5×10^{-11}	Colussi et al. ²³
O(³ P) + NO ₂ → NO ₃	0.9×10^{-31}	2.0	2.2×10^{-11}	DeMore et al. ¹⁵

^a Units are molecule⁻¹ cm³ s⁻¹, $k = A \exp(E/RT)$. ^b Units are molecule⁻² cm⁶ s⁻¹, $k_0 = k_0(298 \text{ K})(T/300)^{-n}$. ^c Value at 312 K.

3. The two reactions appear much more similar in the termolecular channel with the slightly large k_0 value for O(³P) + OClO at 298 K being somewhat compensated by the stronger negative temperature dependence for O(³P) + NO₂.

The patterns of reactivity as reflected in the room-temperature rate coefficient are similar, with two notable exceptions, for the reactions X + OClO and X + O₃ where X = O(³P), NO, OH, SO, Br, Cl, and H. The rate coefficients are summarized in Table 3. The rate coefficients for both the OClO and O₃ reactions, with the two exceptions noted below, increase in the order O(³P) < NO < OH < SO < Br < Cl, H. The reactions which deviate from the pattern and the direction of the deviation are informative. The first exception is that OH + OClO is faster than the trend would suggest. This, however, is consistent with the fact that the rate coefficients listed for all 14 reactions considered, with the exception of OH + OClO, are for reactions in which an O atom is abstracted and which can be represented by X + O₃ → XO + O₂ or X + OClO → XO + ClO. The products of OH + OClO have been shown¹¹ to be primarily HOCl + O₂ and not H₂O + ClO. This suggests the occurrence of an addition–decomposition process which would be expected to differ from the pattern of the other reactions. The second exception involves the reaction pair

TABLE 3: Trends in Room-Temperature Rate Constants for Reactions of Atoms and Free Radicals with OCIO and O₃

X	$k(X + O_3)^a$	$k(X + OCIO)^a$	ref
O(³ P)	8.0×10^{-15}	$1.0 \times 10^{-13}^b$	DeMore et al.; ¹⁵ this work
NO	1.8×10^{-14}	3.4×10^{-13}	DeMore et al. ¹⁵
OH	6.8×10^{-14}	6.8×10^{-12}	DeMore et al. ¹⁵
SO	9.0×10^{-14}	1.9×10^{-12}	DeMore et al. ¹⁵
Br	1.2×10^{-12}	3.4×10^{-13}	DeMore et al. ¹⁵
Cl	1.2×10^{-11}	5.8×10^{-11}	DeMore et al. ¹⁵
H	2.9×10^{-11}	5.7×10^{-11}	DeMore et al.; ¹⁵ Bemand et al. ⁹

^a Rate constant at 298 K in units of molecule⁻¹ cm³ s⁻¹. ^b Low-pressure abstraction channel.

SO + OCIO and Br + OCIO and probably has a less fundamental explanation. It is evident from Table 3 that the order of reactivity is reversed for this pair, being SO < Br for the O₃ reaction and Br < SO for the OCIO reaction. Since independent measurements of both SO + O₃ (three studies) and Br + O₃ (five studies) are in good agreement while the results for Br + OCIO and SO + OCIO are each based on only a single published study, it is worthwhile to review the difficulties reported in these determinations. In the case of Br + OCIO → BrO + ClO, Clyne and Watson¹⁰ monitored the decay of OCIO with Br in excess and encountered serious complications due to reformation of OCIO via the secondary reaction, BrO + ClO. Although considerable effort was made to correct for this, the actual rate coefficient for Br + OCIO could be larger than measured if the treatment for OCIO reformation was not fully adequate. For the reaction SO + OCIO → SO₂ + ClO, Clyne and MacRobert¹² monitored the decay of SO in excess OCIO. They showed that the initial reaction was followed by the rapid chain steps SO + ClO → SO₂ + Cl and Cl + OCIO → 2ClO. Again, major efforts were expended to minimize or allow for this complication including addition of Br₂ as a Cl scavenger, use of initial decay rates, and finally computer fitting of the observed SO decays. In this case, the actual rate coefficient for SO + OCIO could be smaller than measured if the allowance for the secondary chain reaction was insufficient. Thus, the reversal of the trend from SO < Br for the O₃ reactions to Br < SO for the OCIO reaction raises the real possibility that the rate constant for Br + OCIO has been underestimated, the rate coefficient for SO + OCIO has been overestimated, or both.

Acknowledgment. This research was supported by NASA's Upper Atmospheric Research Program. J.F.G. thanks the National Academy of Science/National Research Council for his Resident Research Associateship. The authors thank A. J. Colussi, S. P. Sander, and D. W. Toohey for communicating their data prior to publication.

References and Notes

- (1) Solomon, S.; Mount, G. H.; Sanders, R. W.; Schmeltekopf, A. L. *J. Geophys. Res.* **1987**, *D92*, 8329.
- (2) Sanders, R. W.; Solomon, S.; Carroll, M. A.; Schmeltekopf, A. L. *J. Geophys. Res.* **1989**, *D94*, 11381.
- (3) Wahner, A.; Jakoubek, R. O.; Mount, G. H.; Ravishankara, A. R.; Schmeltekopf, A. L. *J. Geophys. Res.* **1989**, *D94*, 11405.
- (4) Solomon, S.; Mount, G. H.; Sanders, R. W.; Jakoubek, R. O.; Schmeltekopf, A. L. *Science* **1988**, *242*, 550.
- (5) Schiller, C.; Wahner, A.; Platt, U.; Dorn, H. P.; Callies, C.; Ehhalt, D. H. *Geophys. Res. Lett.* **1990**, *17*, 501.
- (6) Wahner, A.; Schiller, C. *J. Geophys. Res.* **1992**, *D97*, 8047.
- (7) Solomon, S.; Sanders, R. W.; Carroll, M. A.; Schmeltekopf, A. L. *J. Geophys. Res.* **1989**, *D94*, 11391.
- (8) Solomon, S.; Sanders, R. W.; Miller, H. L. *J. Geophys. Res.* **1990**, *D95*, 13807.
- (9) Bemand, P. P.; Clyne, M. A. A.; Watson, R. T. *J. Chem. Soc., Faraday Trans. 1* **1973**, *69*, 1356.
- (10) Clyne, M. A. A.; Watson, R. T. *J. Chem. Soc., Faraday Trans. 1* **1977**, *73*, 1169.
- (11) Poulet, G.; Zagogianni, H.; LeBras, G. *Int. J. Chem. Kinet.* **1986**, *18*, 847.
- (12) Clyne, M. A. A.; MacRobert, A. J. *Int. J. Chem. Kinet.* **1981**, *13*, 187.
- (13) Birks, J. W.; Shoemaker, B.; Leck, T. J.; Borders, R. A.; Hart, L. J. *J. Chem. Phys.* **1977**, *66*, 4591.
- (14) Wongdontri-Stuper, W.; Jayanty, R. K. M.; Simonaitis, R.; Hecklen, J. *J. Photochem.* **1979**, *10*, 163.
- (15) DeMore, W. B.; Sander, S. P.; Golden, D. M.; Molina, M. J.; Hampson, R. F.; Kurylo, M. J.; Howard, C. J.; Ravishankara, A. R. *JPL Publ.* **1990**, 90-1.
- (16) Colussi, A. J. *J. Phys. Chem.* **1990**, *94*, 8922.
- (17) Hayman, G. D.; Cox, R. A. *Chem. Phys. Lett.* **1989**, *155*, 1.
- (18) Parr, A. D.; Wayne, R. P.; Hayman, G. D.; Jenkin, M. E.; Cox, R. A. *Geophys. Res. Lett.* **1990**, 2357.
- (19) Brunning, J.; Stief, L. J. *J. Chem. Phys.* **1986**, *84*, 4371.
- (20) Toohey, D. W. Ph.D. Thesis, Harvard University, 1988.
- (21) Wahner, A.; Tyndall, G. S.; Ravishankara, A. R. *J. Phys. Chem.* **1987**, *91*, 2734.
- (22) De More, W. B.; Sander, S. P.; Golden, D. M.; Hampson, R. F.; Kurylo, M. J.; Howard, C. J.; Ravishankara, A. R.; Kolb, C. E.; Molina, M. J. *JPL Publ.* **1992**, 92-20.
- (23) Colussi, A. J.; Sander, S. P.; Friedl, R. R. *J. Phys. Chem.* **1992**, *96*, 4442.
- (24) Troe, J. *J. Phys. Chem.* **1979**, *83*, 114.